J Electr Eng Technol.2017; 12(6): 2365-2377
http://doi.org/10.5370/JEET.2017.12.6.2365

ISSN(Print) 1975-0102
ISSN(Online) 2093-7423

Design of Adaptive Neural Tracking Controller for Pod Propulsion Unmanned Vessel Subject to Unknown Dynamics

Dong-Dong Mu*, Guo-Feng Wang† and Yun-Sheng Fan*

Abstract – This paper addresses two interrelated problems concerning the tracking control of pod propulsion unmanned surface vessel (USV), namely, the modeling of pod propulsion USV, and tracking controller design. First, based on MMG modeling theory, the model of pod propulsion USV is derived. Furthermore, a practical adaptive neural tracking controller is proposed by backstepping technique, neural network approximation and adaptive method. Meanwhile, unlike some existing tracking methods for surface vessel whose control algorithms suffer from "explosion of complexity", a novel neural shunting model is introduced to solve the problem. Using a Lyapunov functional, it is proven that all error signals in the system are uniformly ultimately bounded. The advantages of the paper are that first, the underactuated characteristic of pod propulsion USV is proved; second, the neural shunting model is used to solve the problem of "explosion of complexity", and this is a combination of knowledge in the field of biology and engineering; third, the developed controller is able to capture the uncertainties without the exact information of hydrodynamic damping structure and the sea disturbances. Numerical examples have been given to illustrate the performance and effectiveness of the proposed scheme.

Keywords: Pod, USV, Modeling, Tracking control, Adaptive, Robot and automation

1. Introduction

USV is a kind of small surface movement platform (robot), which has the ability of autonomous navigation in the marine environment, and it can carry out the corresponding tasks by equipping with different functional modules [1]. As a modern robot, USV has a broad application prospect in the military and civil fields. In the military field, it has a great advantage in performing tasks that are dangerous or inappropriate for people to participate in. Meanwhile, it can also be used as a transfer station or collector to work with autonomous underwater vehicles (AUV) [2]. In civilian areas, USV can reduce the personnel expenses and improve the safety of ship navigation. In the complex and changeable ocean environment, USV is able to track the desired path autonomously and quickly, which is the premise and basis for accomplish the task satisfactorily. Tracking control is one of the most important research topics in USV automatic control field.

In order to fulfill the mission In the complex marine environment, it is necessary to maintain a high speed and has a good control characteristic, so this puts forward higher requirements for the propulsion system. Pod is one of the most promising technologies in the field of ship power, which can improve the efficiency and maneuverability of surface vessel [3]. Its essence is a kind of vector propeller, and propulsion and steering function are integrated in pod system. In order to reduce the difficulty of operation and the cost of production, on the basis of the vector propulsion, the propulsion angle is limited to 35 degrees, and this is a pod-like (such as outboard engine and waterjet propulsion) [4]. In order to study the motion control technology of pod propulsion USV, it is necessary to establish its maneuvering motion model.

Recently, the tracking problem of surface vessel has been of great interest. Several tracking controllers have been proposed in the literatures. Based on Lyapunov's direct method and passivity approach, two tracking solutions were proposed in [5] for an underactuated surface ship. However, both in [5] and [6], the yaw velocity should be persistently exciting to guarantee the stability of the control system. Although this limitation was relaxed in [7], the desired trajectory was still constrained by several conditions. In [8], Lyapunov's direct method and back-stepping technique were used to design a controller for an underactuated surface vessels. An adaptive dynamical sliding mode trajectory tracking controller based on backstepping method and dynamical sliding mode control theory was presented in [9]. However, in the aforementioned works, external disturbances were not considered. In [10], an observer was constructed to provide an estimation of unknown disturbances and was applied to design a novel trajectory tracking robust controller through a vectorial backstepping technique. In [11], for underactuated ships in fields of marine practice, adaptive method was used to

† Corresponding Author: School of Information Science and Technology, Dalian Maritime University, China. (gfwangsh@163.com)
* School of Information Science and Technology, Dalian Maritime University, China. (ddmu.phd@gmail.com, yunsheng@dlmu.edu.cn)
Received : March 25, 2017; Accepted : July 6, 2017

compensate for external disturbance. However, the unknown mean external disturbance was assumed to be constant (or at least slowly varying). In [12], neural network with iterative updating laws based on prediction errors was proposed to identify the dynamical uncertainty and time varying ocean disturbances.

It is worth noting that a common assumption in the aforementioned literatures [5-10] around controlling surface vessels is that the model parameters of the controlled surface vessel or its model structure are fully known. However, the actual situations are that: (1) no matter which way to study the model structure of surface vessels, it is based on the assumption and simplification. In other words, many nonlinear terms and unknown parts are omitted, and the structure of the model is uncertain; (2) due to the change of operating conditions, the parameters of the model are also changing at all times. In summary, the previous assumption is not consistent with the actual situation of the project. In order to solve model structure and parameters uncertainty, the task of tracking controller design was attended using the idea of adaptive backstepping with neural network [13-15] or T-S fuzzy system [16-19] based approximation. In [20], a single-layer structure neural network approach was proposed to track control of an autonomous surface vehicle with completely unknown vehicle dynamics and subject to significant uncertainties. In [21], a single-hidden-layer neural network was used to estimate the unstructured uncertainties of a class of uncertain nonlinear systems.

Backstepping method is one of the most popular algorithms, which is employed to design tracking controller for surface vessels [22]. It is considered as an effective design method by constructing both feedback control law and associated Lyapunov function. The advantages of the method to design controller are probably that: (1) all error signals in the system can be easily proved to be uniformly ultimately bounded using Lyapunov functions; (2) the performance of the tracking control strategy can be improved by preserving some nonlinear terms and introducing some functional algorithms compared with the simple feedback linearization technique. However, backstepping control technology has a fatal weakness in the control design that multiple differential of the virtual velocity control signals can lead to "explosion of complexity" phenomenon [23]. Therefore, the final control law is very complex, which not only increases the difficulty of the derivation of the formula, but also to a certain extent increases the amount of calculation of the controller. It is very happy that dynamic surface control (DSC) technique has been proposed in the literature [24] to cope with this aporia by introducing a first-order low pass filter in the process of designing tracking controller. On the basis of [25], DSC technique was introduced into the design of trajectory tracking controllers for underactuated surface ships, which greatly simplifies the complexity of the controller [26].

In this paper, for pod propulsion USV, despite the presence of environmental disturbances induced by wave, wind and ocean-current and unknown dynamics, using backstepping method, neural network approximation, neural shunting model technique and adaptive method design a USV trajectory tracking controller. The main contributions of this note can be summarized as follows:

(1) Under the premise of assumption and simplification, based on the analysis of the propeller thrust force and the force acting on the hull, the pod propulsion USV is proved to be an underactuated system.

(2) The developed tracking controller is universal and model independent, and a novel neural shunting model is introduced to cope the problem of "explosion of complexity".

(3) The control strategy proposed in this paper and some techniques of signal processing are easier to be realized in engineering.

The rest of the paper is organized as follows. Section 2 introduces the derivation process of the model. In Section 3, problem formulation and preliminaries are introduced. In Section 4, tracking controller for underactuated USV is designed. Section 5 proves the stability of controllers and sway direction. In Section 6, case studies are carried out to show the correctness of the control system. Finally, some conclusions are made and future research directions are introduced in Section 7.

2. Modeling of Pod Propulsion USV

The control effect of USV motion controller is not only dependent on the selected control algorithm, but also closely related to the mathematical model. In this section, the model of pod propulsion USV is analyzed in detail to ensure the reliability of controller design and simulation research.

2.1 Kinematics equation

The kinematic equation of USV is used to describe the correspondence between the earth-fixed inertial frame and body-fixed frame.

As shown in Fig. 1, $O-X_0Y_0Z_0$ is the earth-fixed inertial frame and $o-x_0y_0z_0$ is the body-fixed frame. In actual navigation, the motion state of USV consists of 6 degree of freedoms (DOFs) including the surge velocity u, sway velocity v, heave velocity w, yaw rate r, rolling rate p and pitching angle q. However, based on the previous experience, too complex or too simple models is difficult to describe the movement characteristics of USV. In this article, only the horizontal movement of USV is considered. That means that heave velocity, rolling rate and pitching angle are ignored. δ is propulsion angle and (x, y) represents the position of the USV in the earth-fixed inertial frame. The kinematics equation transformation

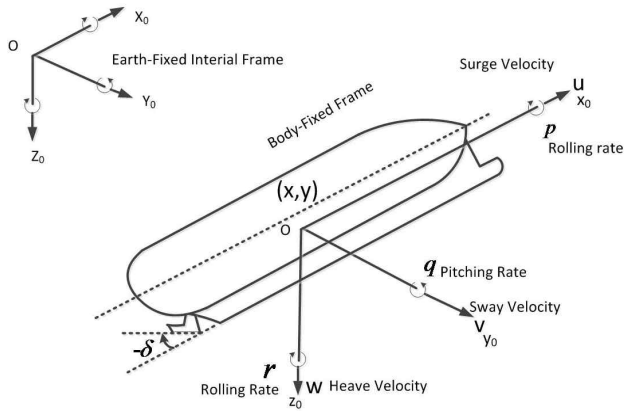

Fig. 1. The corresponding coordinate systems

between the earth-fixed inertial frame and the body-fixed frame can be expressed as

$$\dot{\eta} = J(\psi)\upsilon \tag{1}$$

Where ψ is course angle, $\eta = [\mathrm{x, y, }\psi]^T$ and $\upsilon = [\mathrm{u, v, r}]^T$.

$J(\psi)$ is transformation matrix.

$$J(\psi) = \begin{bmatrix} \cos(\psi) & -\sin(\psi) & 0 \\ \sin(\psi) & \cos(\psi) & 0 \\ 0 & 0 & 1 \end{bmatrix} \tag{2}$$

Then we can get the kinematics equation of USV.

$$\begin{cases} \dot{x} = u\cos\psi - v\sin\psi \\ \dot{y} = u\sin\psi + v\cos\psi \\ \dot{\psi} = r \end{cases} \tag{3}$$

2.2 Kinetic equation

Planar kinetic equation of 3 DOFs is established by Lagrange mechanics theory [27].

$$M\dot{\upsilon} + C(\upsilon)\upsilon + D(\upsilon)\upsilon = \tau \tag{4}$$

where M is inertia matrix, $C(\upsilon)$ is Coriolis and centripetal matrix, $D(\upsilon)$ is Hydrodynamic Damping Matrix. For fully driven vessel, because it is equipped with side thruster, $\tau = [\tau_u, \tau_v, \tau_r]^T$. For underactuated vessel, $\tau_v = 0$. τ_u and τ_r are longitudinal and steering thrust, respectively. M, $C(\upsilon)$ and $D(\upsilon)$ are shown in Eqs.(5), (6) and (7).

$$M = \begin{bmatrix} m - X_{\dot{u}} & 0 & 0 \\ 0 & m - Y_{\dot{v}} & mx_g - Y_{\dot{r}} \\ 0 & mx_g - Y_{\dot{r}} & I_z - N_{\dot{r}} \end{bmatrix} \tag{5}$$

$$C(\upsilon) = \begin{bmatrix} 0 & 0 & a_{13} \\ 0 & 0 & a_{23} \\ a_{31} & a_{32} & 0 \end{bmatrix} \tag{6}$$

$$D(\upsilon) = \begin{bmatrix} -X_u & 0 & 0 \\ 0 & -Y_v & -Y_r \\ 0 & -N_v & -N_r \end{bmatrix} \tag{7}$$

where

$a_{13} = -(m - Y_{\dot{v}})v - (mx_g - Y_{\dot{r}})r$, $a_{23} = (\mathrm{m} - \mathrm{X}_{\dot{u}})\,\mathrm{u}$,
$a_{31} = (m - Y_{\dot{v}})v + (mx_g - Y_{\dot{r}})r$ and $a_{32} = -(m - X_{\dot{u}})u$,

m is the mass of the USV, I_z is the moment of inertia of the o_z axis, x_g is the distance from the barycenter of USV to the body-fixed frame. Besides, the detailed meaning of each parameters can refer to literature [35]. In [14], the thrust of propulsor can be expressed as

$$T = cV\delta_n + d\left|\delta_n\right|\delta_n \tag{8}$$

where T is propulsor thrust, δ_n is the rotate speed of propeller, V is the speed of USV, $c > 0$ and $d > 0$ are the coefficients. When the propulsion angle is δ, the vector thrust in different directions are

$$\begin{cases} X_P = (cV\delta_n + d\left|\delta_n\right|\delta_n)\cos\delta \\ Y_P = (cV\delta_n + d\left|\delta_n\right|\delta_n)\sin\delta \\ N_P = x_p(cV\delta_n + d\left|\delta_n\right|\delta_n)\sin\delta \end{cases} \tag{9}$$

where x_p is the longitudinal moment arm from the center of rotation to the pivot point of the propulsor. According to [28], if δ is small and $x_p > 1$, then we can assume that $Y_p \approx 0$. Define $X_p = \tau_u$ and $N_p = \tau_r$. Then Eq. (4) can be converted to (10).

$$\begin{bmatrix} (m - X_{\dot{u}})\dot{u} \\ (m - Y_{\dot{v}})\dot{v} + (mx_g - Y_{\dot{r}})\dot{r} \\ (mx_g - Y_{\dot{r}})\dot{v} + (I_z - N_{\dot{r}})\dot{r} \end{bmatrix} + \begin{bmatrix} -X_u u + (-(m - Y_{\dot{v}})v - (mx_g - Y_{\dot{r}})r)r \\ -Y_v v + (-Y_r + (m - x_{\dot{u}})u)r \\ ((m - Y_{\dot{v}})vu + (mx_g - Y_{\dot{r}})ru - N_v v - \\ (m - X_{\dot{u}})uv - N_r r) \end{bmatrix} = \begin{bmatrix} \tau_u \\ 0 \\ \tau_r \end{bmatrix} \tag{10}$$

Define $m_{11} = m - X_{\dot{u}}$, $m_{22} = m - Y_{\dot{v}}$, $m_{23} = mx_g - Y_{\dot{r}}$, $m_{32} = mx_g - N_{\dot{v}}$, $m_{33} = I_z - N_{\dot{r}}$, $d_{11} = -X_u$, $d_{22} = -Y_v$, $d_{23} = -Y_r$, $d_{32} = -N_v$, $d_{33} = -N_r$. Then Eq. (10) can be reduced to (11).

$$\begin{bmatrix} m_{11}\dot{u} \\ m_{22}\dot{v}+m_{23}\dot{r} \\ m_{32}\dot{v}+m_{33}\dot{r} \end{bmatrix}+\begin{bmatrix} d_{11}u-m_{22}vr-m_{23}r^2 \\ d_{22}v-d_{23}r+m_{11}ur \\ (m_{22}vu+m_{23}ru+d_{32}v \\ -m_{11}uv+d_{33}r) \end{bmatrix}=\begin{bmatrix} \tau_{\mathrm{u}} \\ 0 \\ \tau_r \end{bmatrix} \tag{11}$$

Assuming that USV is symmetrical and the barycenter of USV coincides with the center of body-fixed frame. This is to say that $x_g=0$, $Y_{\dot{r}}=0$, $N_{\dot{v}}=0$, $Y_r=0$ and $N_v=0$. So, we can simplify the Eq. (11) to (12).

$$\begin{cases} \dot{u}=f_u+\dfrac{1}{m_{11}}\tau_u+\dfrac{1}{m_{11}}b_u \\ \dot{v}=f_v+\dfrac{1}{m_{22}}b_v \\ \dot{r}=f_r+\dfrac{1}{m_{33}}\tau_r+\dfrac{1}{m_{33}}b_r \end{cases} \tag{12}$$

where

$$f_u=\frac{m_{22}}{m_{11}}vr-\frac{d_{11}}{m_{11}}u$$

$$f_v=-\frac{m_{11}}{m_{22}}ur-\frac{d_{22}}{m_{22}}v$$

$$f_r=\frac{m_{11}-m_{22}}{m_{33}}uv-\frac{d_{33}}{m_{33}}r$$

b_u, b_v and b_r are used to describe immeasurable external disturbance forces and moments due to wind, wave and ocean current in the body-fixed frame, respectively. Thus it can be seen that although the pod belongs to vector propulsion, essentially, the pod propulsion USV belongs to underactuated ships. This theory can also be extended to general vector propulsion ships.

Assumption 1. Assume that the disturbance terms satisfy $|b_u|\le b_{u\max}$, $|b_v|\le b_{v\max}$ and $|b_r|\le b_{\mathrm{r}\max}$, Where $b_{u\max}$, $b_{\mathrm{v}\max}$ and $b_{\mathrm{r}\max}$ are unknown positive constants.

Assumption 2. There exist constraints on the control inputs and velocities as $|\tau_u|\le\tau_{u\max}$, $|\tau_r|\le\tau_{\mathrm{r}\max}$, $u\le u_{\max}$, $v\le v_{\max}$ and $r\le r_{\max}$ with positive constants $\tau_{u\max}$, $\tau_{\mathrm{r}\max}$, $u_{\max}$, $v_{\max}$ and $r_{\max}$.

3. Problem Formulation and Preliminaries

This section first briefly describes the control objective. Then, the corresponding problem of tracking control is formulated. The RBF neural network approximation and the neural shunting model are finally outlined.

3.1 Problem formulation

Due to the continuous change of working condition, f_u, f_v and f_r are uncertain. On the other hand, we make a lot of assumptions and ignore a lot of nonlinear terms, so it is more difficult to use precise structure or parameters to express the model of USV.

Control objective: Under this circumstance, the hydrodynamic terms, the modeled dynamics and the marine external disturbance are unknown. The control objective is to develop an adaptive neural tracking controller for underactuated USV to track a specific trajectory $[x_d \quad y_d \quad \psi_d]$.

Where $(x_d \quad y_d)$ is a target point, and $\psi_d\in[0,2\pi)$. The functional relationship between them is

$$\begin{cases} x_d=u_d\cos(\psi_d) \\ y_d=u_d\sin(\psi_d) \\ \dot{\psi}_d=r_d \end{cases}$$

where all variables have similar meanings to (3).

Assumption 3. The reference path or trajectory of the target is regular and smooth enough. x_d, $\dot{x}_d$, $\ddot{x}_d$, y_d, $\dot{y}_d$, $\ddot{y}_d$, ψ_d and $\ddot{\psi}_d$ are all bounded.

Lemma 1. $\forall\partial>0$, there exists a smooth function $\Xi(\cdot)$, $\Xi(0)=0$ and $|\xi|\le\xi\Xi(\xi)+\partial$, $\forall\xi\in\Re$.

Remark 1. A simple example function satisfies Lemma 1 is $\Xi(\xi)=[1/(4\partial)]\xi$ [5].

Remark 2. The passive-bound stable of sway velocity v is proved in [29].

3.2 Nonlinear function approximation

In engineering application, RBF neural network is introduced to approximate the uncertainty of the model. It can be described as $W^T\varphi(x)$ with weight vector $W\in R^q$, note number q, input vector $\mathrm{x}\in\Omega\in R^n$ and basis function vector $\varphi(x)\in R^q$. Universal approximation results indicate that if q is chosen to be sufficiently large, then $W^T\varphi(x)$ can approximate any continuous nonlinear function. The network structure is shown in Fig. 2.

Define a continuous function $f(\mathrm{x})$, RBF neural network is used to approximate function $f(\mathrm{x})$.

$$f(x)=W^T\varphi(x)+\varepsilon \qquad \forall x\subset\Omega_x \tag{13}$$

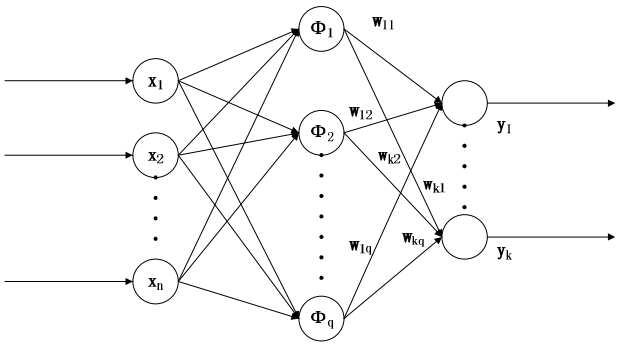

Fig. 2. RBF neural network structure

where the weight vector $W=\left[w_1,w_2,....,w_q\right]^T\in R^q$, ε is the approximation error, the neural network node number $q>1$ and $\varphi(x)=\left[\varphi_1(x),\varphi_2(x),....,\varphi_q(x)\right]^T$, with $\varphi_i(x)$ being chosen as the commonly used Gaussian function, which have the from

$$\varphi_i(x)=\exp\left[-\frac{(x-c_i)^T(x-c_i)}{2\sigma_i^2}\right],i=1,2,....,q \tag{14}$$

where $\mathrm{x}=\left[x_1,x_2,....,x_n\right]$ is the input samples, $c_i=\left[c_{i1},c_{i2},....,c_{in}\right]$ is the center of the receptive field and σ_{i} is the width of the Gaussian function. The output of the network can be described as

$$y_k=\sum_{i=1}^{q}w_{ki}\varphi_i(\left\|x-c_i\right\|^2),i=1,2,3,....,q \tag{15}$$

where y_k is the output of k node of the output layer. According to [30], it has been proven that $f(\mathrm{x})$ can be approximated to arbitrary any accuracy with the ideal constant weights:

$$W^{*T}:=\arg\min_{W\subset R^q}\left\{\sup_{x\subset\Omega_x}\left|f(x)-W^T\varphi(x)\right|\right\}$$

where W^{*T} is the ideal constant weights. The function approximation error ε of neural network is bounded by

$$\left\|W^*\right\|\le W_{\mathrm{m}},\left|\varepsilon\right|\le\varepsilon_{\mathrm{m}}\qquad\forall x\subset\Omega_x$$

where W_m and ε_m are positive constants. It is worth mentioning that in the following sections, $\hat{(\bullet)}$ is the estimate value of $(\bullet)$, and the estimate error $\tilde{(\bullet)}=\hat{(\bullet)}-(\bullet)$. $\left|\bullet\right|$ is the absolute operator and $\left\|\bullet\right\|$ denotes the Euclidean norm.

3.3 Neural shunting model

As everyone knows, the neuron is the basic unit of the structure and function of the nervous system, and it has the function of feeling stimulation and transmitting signal. According to its biological characteristics and circuit theory, Hodgkin and Huxley [26] proposed a model for a patch of membrane in a biological neural system using electrical circuit elements. This modeling work together with other experimental work led them to win a Nobel Prize in 1963. In their membrane model, the dynamics of voltage across the membrane can be described using the state equation technique as

$$C_m\dot{V}_m=-(E_p+V_m)g_p+(E_{Na}-V_m)g_{Na}-(E_k+V_m)g_K \tag{16}$$

where V_m is the membrane voltage, C_m is the membrane capacitance. Parameters E_p, E_k and E_{Na} are the saturation potentials for potassium ions, sodium ions and the passive leak current in the membrane, respectively. Parameters g_p, g_{Na} and g_K represent the conductance of potassium, sodium and passive channel, respectively.

Define $C_m=1$, $\chi_i=E_p+V_m$, $A=g_p$, $B=E_{Na}+E_p$, $D=E_k-E_p$, $S_i^+=g_{Na}$ and $S_i^-=g_K$. Then Eq. (16) can be changed into a typical neural shunting model.

$$\dot{\chi}_i=-A\chi_i+(B-\chi_i)S_i^+(t)-(D+\chi_i)S_i^-(t) \tag{17}$$

where χ_i is the neural activity of the i th neuron. A, B and D are normal numbers, representing the passive decay rate, the upper bound and lower bound of the neural activity. S_i^- is the total external negative input to the neuron called inhibitory input and S_i^+ is the total external positive input to the neuron called excitatory input. This neural shunting model was proposed by Grossberg in 1988, and it was used to understand the real-time adaptive response of an individual to a complex and dynamic environment. At the same time, with the development of control theory, the neural shunting model has been applied in many fields, such as biology, machine vision, robot control, path planning and so on. This paper studies the application of the neural shunting model to the tracking control of pod propulsion USV.

Remark 3. Neuron output potential χ_i is continuous and smooth. It varies with the excitation input and the inhibitory input.

Remark 4. Neuron output potential χ_i is limited to the range of $[-D,B]$.

4. Control Design

In order to realize the tracking control of underactuated USV, a practical adaptive control law is proposed in this chapter. The design procedure contains two steps: design of surge motion and design of yaw motion.

4.1 Design of surge motion

The USV's yaw motion is treated independently from surge and sway motions. First, the error variables are defined as follows:

$$\begin{cases}x_e=x_d-x\\y_e=y_d-y\\z_e=\sqrt{x_e^2+y_e^2}\\\psi_e=\psi_d-\psi\end{cases} \tag{18}$$

and

$$\psi_d=\arctan(y_e/x_e)+0.5\cdot\pi[1-\mathrm{sgn}(x_e)]\mathrm{sgn}(y_e) \tag{19}$$

It is worth noting that if $z_e = 0$, we define that ψ_d takes its previous value and $\dot{\psi}_d = \ddot{\psi}_d = 0$. Referring to Eq. (18), we can get the following equation:

$$\begin{cases} x_e = z_e \cos\psi_d \\ y_e = z_e \sin\psi_d \end{cases} \tag{20}$$

The virtual control law α_u is selected as

$$\alpha_u = \frac{k_{ze} z_e + \dot{x}_d \cos\psi_d + \dot{y}_d \sin\psi_d - v\sin\psi_e}{\cos\psi_e} \tag{21}$$

where $k_{ze} \geq 0$ is a positive parameter.

Note that the α_u is not defined when $\psi_e = \pm\frac{\pi}{2}$. Therefore in the process of designing the controller, requires $|\psi_e| < \frac{\pi}{2}$. In order to facilitate the implementation of the project, it is necessary to carry out the relevant transformation, and the transformation does not change the virtual control direction. The corresponding transformation rules are that if $\psi_e \geq \frac{\pi}{2}$, $\psi_e = \psi_e - \pi$; if $-\frac{\pi}{2} < \psi_e < \frac{\pi}{2}$, $\psi_e = \psi_e$; if $\psi_e \leq -\frac{\pi}{2}$, $\psi_e = \psi_e + \pi$. In other words, through the above transformation, the scope of error variable ψ_e is $(-\frac{\pi}{2}, \frac{\pi}{2})$.

To avoid the differential of α_u, let α_u pass through the neural shunting model.

$$\dot{\beta}_u = -A_1\beta_u + (B_1 - \beta_u) f(\alpha_u) - (D_1 + \beta_u) g(\alpha_u) \tag{22}$$

where A_1, B_1 and D_1 have the same meanings as those defined in (17).

Define

$$u_e = u - \beta_u \tag{23}$$

Differentiating (23), and substituting (12) and (22) into it, we have

$$\dot{u}_e = \dot{u} - \dot{\beta}_u = f_u + \frac{1}{m_{11}}\tau_u + \frac{1}{m_{11}} b_u + \Theta_u \tag{24}$$

where

$$\Theta_u = ([A_1 + f(\alpha_u) + g(\alpha_u)]\beta_u - [B_1 f(\alpha_u) - D_1 g(\alpha_u)]).$$

It is easy to see that Eq. (24) is in a well-known strict-feedback form. Meanwhile, for unknown or uncertain dynamics, define

$$f_u = \hat{f}_u(Z_u) + \varepsilon_u \tag{25}$$

where $Z_u = [u, v, r]$, ε_u is the approximation error with unknown upper bound $\bar{\varepsilon}_u$. The corresponding control law is chosen as

$$\tau_u = -k_{ue} u_e - m_{11}\hat{f}_u - \hat{b}_u \phi(u_e) - m_{11}\Theta_u - z_e \cos\psi_e \tag{26}$$

where k_{ue} is a parameter greater than zero, $\hat{b}_u$ is the estimated value of b_u, and its error $\tilde{b}_u = \hat{b}_u - b_u$. Finally, the update law for the neural network weights and the estimated upper bound of external disturbance are taken to be

$$\dot{\hat{W}}_u = \Gamma_u [u_e m_{11} \varphi(Z_u) - \sigma_u (\hat{W}_u - \hat{W}_u(0))] \tag{27}$$

$$\dot{\hat{b}}_{u\max} = \gamma_u [u_e \phi(u_e) - \sigma_{bu} (\hat{b}_{u\max} - \hat{b}_{u\max 0})] \tag{28}$$

where Γ_u, σ_u, γ_u, σ_{bu} are positive design parameters. $\hat{W}_u(0)$ and $\hat{b}_{u\max 0}$ are the initial value of the related variables.

4.2 Design of yaw motion

The yaw moment τ_r is designed individually for the purpose of stabilizing tracking error ψ_e.

Substituting (18) into (12), error dynamics of the yaw motion can be rewritten as following.

$$\dot{\psi}_e = \dot{\psi}_d - r \tag{29}$$

The virtual control law α_r is selected as

$$\alpha_r = \dot{\psi}_d + k_{\psi e}\psi_e \tag{30}$$

where $k_{\psi e} \geq 0$ is a positive parameter.

Remark 5. We noticed that α_r contains $\dot{\psi}_d$ items. In practical engineering, all signals are discrete, so in order to be closer to reality, $\dot{\psi}_d = (\psi_d(t) - \psi_d(t-1))/\Delta t$. In this paper, $\Delta t = 0.01$. For special cases, some additional transformations also require to be conducted to calculate the variable $\dot{\psi}_d$. Such as if $\psi_d(t-1)$ is 0 degree and $\psi_d(t)$ is 359 degrees, suing the above method, we can get that $\dot{\psi}_d = (\psi_d(t) - \psi_d(t-1) - 360^\circ)/\Delta t$.

To avoid the differential of α_r, let α_r pass through neural shunting model.

$$\dot{\beta}_r = -A_2\beta_r + (B_2 - \beta_r) f(\alpha_r) - (D_2 + \beta_r) g(\alpha_r) \tag{31}$$

Where A_2, B_2 and D_2 have the same meanings as those defined in (17).

Define

$$r_e = r - \beta_r \tag{32}$$

Differentiating (32), and substituting (12) and (31) into it, we have

$$\dot{r}_e = \dot{r} - \dot{\beta}_r = f_r + \frac{1}{m_{33}}\tau_r + \frac{1}{m_{33}}b_r + \Theta_r \tag{33}$$

where

$$\Theta_r = ([A_2 + f(\alpha_r) + g(\alpha_r)]\beta_r - [B_2 f(\alpha_r) - D_2 g(\alpha_r)]) .$$

Similar to the previous discussion, define

$$f_r = \hat{f}_r(Z_r) + \varepsilon_r \tag{34}$$

where $Z_r = [u, v, r]$, ε_r is the approximation error with unknown upper bound $\bar{\varepsilon}_r$. The corresponding control law for (32) is chosen as

$$\tau_r = -k_{re} r_e - m_{33}\hat{f}_r - \hat{b}_r \phi(r_e) - m_{33}\Theta_r - \psi_e \tag{35}$$

Where k_{re} is a parameter greater than zero, $\hat{b}_r$ is the estimated value of b_r, and its error $\tilde{b}_r = \hat{b}_r - b_r$. Finally, the update law for the RBF neural network weights and the estimated upper bound of external disturbance are taken to be

$$\dot{\hat{W}}_r = \Gamma_r[r_e m_{33}\varphi(Z_r) - \sigma_r(\hat{W}_r - \hat{W}_r(0))] \tag{36}$$

$$\dot{\hat{b}}_{r\max} = \gamma_r[r_e \phi(r_e) - \sigma_{br}(\hat{b}_{r\max} - \hat{b}_{r\max 0})] \tag{37}$$

where Γ_r, σ_r, γ_r σ_{br} are positive design parameters. $\hat{W}_r(0)$ and $\hat{b}_{r\max 0}$ are the initial value of the related variables.

Compared with the works in [22] and [32], the advantages of this paper are that it does not need the information around the hydrodynamic terms, unmodeled dynamics due to the online approximation capability of RBF neural network. At the same time, in assumption 2, we assume that the external disturbances are bounded. We must adopt certain methods to deal with the disturbances, so an adaptive method is used to compensate the unknown external disturbances.

Remark 6. As mentioned in the literature [11], RBF neural network is only used to process the uncertain functions f_u and f_r. The control gain coefficients $\frac{1}{m_{11}}$ and $\frac{1}{m_{33}}$ are not being approached. Based on past experience, the estimation of a constant is not satisfactory. In order to avoid the potential control singularity problem, it is advisable to the control gain without being approached.

5. Stability Analysis

Theorem 1. Consider the closed-loop system consisting of the USV dynamics (3), (12), the control laws (26), (35), the RBF neural network adaptive update laws (27), (36), the neural shunting models (22), (31) together with the disturbance adaptive update laws (28), (37). There exist appropriate design parameters k_{ze}, k_{ue}, $k_{\psi e}$, k_{re}, Γ_u, σ_u, γ_u, σ_{bu}, Γ_r, σ_r, γ_r, σ_{br} such that all error signals in the system are uniformly ultimately bounded (UUB).

Define

$$y_u = \beta_u - \alpha_u \tag{38}$$

Differentiating (38), and substituting (21) and (22) into it, we have

$$\begin{aligned}\dot{y}_u &= \dot{\beta}_u - \dot{\alpha}_u \\ &= -([A_1 + f(\alpha_u) + g(\alpha_u)]\beta_u - [B_1 f(\alpha_u) \\ &\quad - D_1 g(\alpha_u)]) - \mathrm{X}_1\end{aligned} \tag{39}$$

where

$$\begin{aligned}\mathrm{X}_1 &= \frac{\partial \alpha_u}{\partial x}\dot{x} + \frac{\partial \alpha_u}{\partial y}\dot{y} + \frac{\partial \alpha_u}{\partial \psi}\dot{\psi} + \frac{\partial \alpha_u}{\partial x_d}\dot{x}_d \\ &+ \frac{\partial \alpha_u}{\partial y_d}\dot{y}_d + \frac{\partial \alpha_u}{\partial \psi_r}\dot{\psi}_r + \frac{\partial \alpha_u}{\partial \dot{x}_d}\ddot{x}_d + \frac{\partial \alpha_u}{\partial \dot{y}_d}\ddot{y}_d + \frac{\partial \alpha_u}{\partial v}\dot{v}\end{aligned} \tag{40}$$

Meanwhile, from the definition of $f(\alpha_u)$ and $g(\alpha_u)$ can be seen that $f(\alpha_u) > 0$ and $g(\alpha_u) > 0$. If $\alpha_u > 0$, $f(\alpha_u) = \alpha_u$ and $g(\alpha_u) = 0$; if $\alpha_u < 0$, $f(\alpha_u) = 0$ and $g(\alpha_u) = -\alpha_u$. Therefore, if $B_1 = D_1$, the Eq. (39) is simplified as

$$\dot{y}_u = \dot{\beta}_u - \dot{\alpha}_u = -A_u\beta_u + B_1\alpha_u - \mathrm{X}_1 \tag{41}$$

where $A_u = A_1 + f(\alpha_u) + g(\alpha_u)$.

Similarly, define

$$y_r = \beta_r - \alpha_r \tag{42}$$

Differentiating (42), and substituting (30) and (31) into it, we have

$$\begin{aligned}\dot{y}_r = \dot{\beta}_r - \dot{\alpha}_r &= -([A_2 + f(\alpha_r) + g(\alpha_r)]\beta_r \\ &\quad -[B_2 f(\alpha_r) - D_2 g(\alpha_r)]) - \mathrm{X}_2\end{aligned} \tag{43}$$

where

$$\mathrm{X}_2 = \frac{\partial \alpha_r}{\partial \psi}\dot{\psi} + \frac{\partial \alpha_r}{\partial \psi_r}\dot{\psi}_r + \frac{\partial \alpha_r}{\partial \dot{\psi}_r}\ddot{\psi}_r \tag{44}$$

Similar to previous, if $B_2 = D_2$, the Eq. (43) is simplified as

$$\dot{y}_r = \dot{\beta}_r - \dot{\alpha}_r = -A_r\beta_r + B_2\alpha_r - \mathrm{X}_2 \tag{45}$$

where $A_r = A_2 + f(\alpha_r) + g(\alpha_r)$.

Remark 7. X_1 and X_2 are bounded, and we assume that $X_1 \le \bar{X}_1$ and $X_2 \le \bar{X}_2$. Where $\bar{X}_1$ and $\bar{X}_2$ are normal numbers greater than zero.

Proof. Consider the following Lyapunov function candidate.

$$V = \frac{1}{2}(z_e^2 + \psi_e^2 + m_{11}u_e^2 + m_{33}r_e^2 + y_u^2 + y_r^2 + \tilde{W}_u^T\Gamma_u^{-1}\tilde{W}_u + \tilde{W}_r^T\Gamma_r^{-1}\tilde{W}_r + \gamma_u^{-1}\tilde{b}_{u\max}^2 + \gamma_r^{-1}\tilde{b}_{r\max}^2) \quad (46)$$

Take the time derivative $\dot{V}$ along (20), (24), (29), (33), and submitting the control laws (26) and (35), we have

$$\begin{aligned}\dot{V} \le & -k_{ze}z_e^2 - k_{\psi e}\psi_e^2 - (k_{ue} - \frac{1}{2})u_e^2 - (k_{re} - \frac{1}{2})r_e^2 \\ & -\tilde{W}_u^T(u_e m_{11}\varphi(Z_u) - \Gamma_u^{-1}\dot{\hat{W}}_u) - \tilde{W}_r^T(r_e m_{33}\varphi(Z_r) - \Gamma_r^{-1}\dot{\hat{W}}_r) \\ & -\tilde{b}_{u\max}(u_e\phi(u_e) - \gamma_u^{-1}\dot{\hat{b}}_{u\max}) - \tilde{b}_{r\max}(r_e\phi(r_e) - \gamma_r^{-1}\dot{\hat{b}}_{r\max}) \\ & +u_e b_u - u_e b_{u\max}\phi(u_e) + r_e b_r - r_e b_{r\max}\phi(r_e) + \frac{1}{2}\bar{\varepsilon}_u^2 + \frac{1}{2}\bar{\varepsilon}_r^2 \\ & +y_u\dot{y}_u + y_r\dot{y}_r\end{aligned}$$

Submitting the adaptive laws (27), (28), (36) and (37) yields

$$\begin{aligned}\dot{V} \le & -k_{ze}z_e^2 - k_{\psi e}\psi_e^2 - (k_{ue} - \frac{1}{2})u_e^2 - (k_{re} - \frac{1}{2})r_e^2 \\ & -\sigma_u\tilde{W}_u^T(\hat{W}_u - \hat{W}_u(0)) - \sigma_r\tilde{W}_r^T(\hat{W}_r - \hat{W}_r(0)) \\ & -\sigma_{bu}\tilde{b}_{u\max}(\hat{b}_{u\max} - \hat{b}_{u\max 0}) - \sigma_{br}\tilde{b}_{r\max}(\hat{b}_{r\max} - \hat{b}_{r\max 0}) \\ & +u_e b_u - u_e b_{u\max}\phi(u_e) + r_e b_r - r_e b_{r\max}\phi(r_e) + \frac{1}{2}\bar{\varepsilon}_u^2 + \frac{1}{2}\bar{\varepsilon}_r^2 \\ & +y_u\dot{y}_u + y_r\dot{y}_r\end{aligned}$$

From Young's inequality, we have

$$-\tilde{W}_i^T(\hat{W}_i - \hat{W}_i(0)) \le -\frac{\left\|\tilde{W}_i\right\|^2}{2} + \frac{\left\|W_i - \hat{W}_i(0)\right\|^2}{2}$$

$$-\tilde{b}_{i\max}(\hat{b}_{i\max} - \hat{b}_{i\max 0}) \le -\frac{\tilde{b}_i^2}{2} + \frac{(b_i - \hat{b}_{i\max 0})^2}{2}$$

where $i = u$ and r. Then

$$\begin{aligned}\dot{V} \le & -k_{ze}z_e^2 - k_{\psi e}\psi_e^2 - (k_{ue} - \frac{1}{2})u_e^2 - (k_{re} - \frac{1}{2})r_e^2 \\ & -\sigma_u\frac{\left\|\tilde{W}_u\right\|^2}{2} - \sigma_r\frac{\left\|\tilde{W}_r\right\|^2}{2} - \sigma_{bu}\frac{\tilde{b}_{u\max}^2}{2} - \sigma_{br}\frac{\tilde{b}_{r\max}^2}{2} \\ & +\sigma_u\frac{\left\|W_u - \hat{W}_u(0)\right\|^2}{2} + \sigma_r\frac{\left\|W_r - \hat{W}_r(0)\right\|^2}{2} \\ & +\sigma_{bu}\frac{(b_{u\max} - \hat{b}_{u\max 0})^2}{2} + \sigma_{br}\frac{(b_{r\max} - \hat{b}_{r\max 0})^2}{2} \\ & +\partial(b_{u\max} + b_{r\max}) + \frac{1}{2}\bar{\varepsilon}_u^2 + \frac{1}{2}\bar{\varepsilon}_r^2 + y_u\dot{y}_u + y_r\dot{y}_r\end{aligned}$$

Submitting the Eqs. (41) and (45) yields

$$\begin{aligned}\dot{V} \le & -k_{ze}z_e^2 - k_{\psi e}\psi_e^2 - (k_{ue} - \frac{1}{2})u_e^2 - (k_{re} - \frac{1}{2})r_e^2 \\ & -\sigma_u\frac{\left\|\tilde{W}_u\right\|^2}{2} - \sigma_r\frac{\left\|\tilde{W}_r\right\|^2}{2} - \sigma_{bu}\frac{\tilde{b}_{u\max}^2}{2} - \sigma_{br}\frac{\tilde{b}_{r\max}^2}{2} \\ & +\sigma_u\frac{\left\|W_u - \hat{W}_u(0)\right\|^2}{2} + \sigma_r\frac{\left\|W_r - \hat{W}_r(0)\right\|^2}{2} \\ & +\sigma_{bu}\frac{(b_{u\max} - \hat{b}_{u\max 0})^2}{2} + \sigma_{br}\frac{(b_{r\max} - \hat{b}_{r\max 0})^2}{2} \\ & +\partial(b_{u\max} + b_{r\max}) - y_u(A_u\beta_u - B_1\alpha_u) + \frac{1}{2}\bar{\varepsilon}_u^2 \\ & +\frac{1}{2}\bar{\varepsilon}_r^2 - y_r(A_r\beta_r - B_2\alpha_r) - y_u X_1 - y_r X_2\end{aligned}$$

Define $B_1 = A_u$ and $B_2 = A_r$.
Then $A_u\beta_u - A_u\alpha_u = A_u y_u$, $A_r\beta_r - A_r\alpha_r = A_r y_r$. So

$$\begin{aligned}\dot{V} \le & -k_{ze}z_e^2 - k_{\psi e}\psi_e^2 - (k_{ue} - \frac{1}{2})u_e^2 - (k_{re} - \frac{1}{2})r_e^2 \\ & -\sigma_u\frac{\left\|\tilde{W}_u\right\|^2}{2} - \sigma_r\frac{\left\|\tilde{W}_r\right\|^2}{2} - \sigma_{bu}\frac{\tilde{b}_{u\max}^2}{2} - \sigma_{br}\frac{\tilde{b}_{r\max}^2}{2} \\ & +\sigma_u\frac{\left\|W_u - \hat{W}_u(0)\right\|^2}{2} + \sigma_r\frac{\left\|W_r - \hat{W}_r(0)\right\|^2}{2} \\ & +\sigma_{bu}\frac{(b_{u\max} - \hat{b}_{u\max 0})^2}{2} + \sigma_{br}\frac{(b_{r\max} - \hat{b}_{r\max 0})^2}{2} \\ & +\partial(b_{u\max} + b_{r\max}) - A_u y_u^2 - A_r y_r^2 + \frac{1}{2}\bar{\varepsilon}_u^2 + \frac{1}{2}\bar{\varepsilon}_r^2 \\ & -y_u X_1 - y_r X_2\end{aligned}$$

Form Young's inequality, i.e.,

$ab \le \frac{1}{2\sigma}a^2 + \frac{\sigma}{2}b^2$ with $\sigma > 0$ and $(a,b) \in \Re^2$, it follows that

$$-y_u X_1 \le \frac{\sigma_{yu}y_u^2}{2} + \frac{\bar{X}_1^2}{2\sigma_{yu}}$$

$$-y_r X_2 \le \frac{\sigma_{yr}y_r^2}{2} + \frac{\bar{X}_2^2}{2\sigma_{yr}}$$

Where σ_{yu} and σ_{yr} are arguments greater than zero. Then

$$\begin{aligned}\dot{V} \le & -k_{ze}z_e^2 - k_{\psi e}\psi_e^2 - (k_{ue} - \frac{1}{2})u_e^2 - (k_{re} - \frac{1}{2})r_e^2 \\ & -\sigma_u \frac{\left\|\tilde{W}_u\right\|^2}{2} - \sigma_r \frac{\left\|\tilde{W}_r\right\|^2}{2} - \sigma_{bu} \frac{\tilde{b}_{u\max}^2}{2} - \sigma_{br} \frac{\tilde{b}_{r\max}^2}{2} \\ & -(A_u - \frac{\sigma_{yu}}{2})y_u^2 - (A_r - \frac{\sigma_{yr}}{2})y_r^2 + \sigma_u \frac{\left\|W_u - \hat{W}_u(0)\right\|^2}{2} \\ & +\sigma_r \frac{\left\|W_r - \hat{W}_r(0)\right\|^2}{2} + \sigma_{bu} \frac{(b_{u\max} - \hat{b}_{u\max 0})^2}{2} \\ & +\sigma_{br} \frac{(b_{r\max} - \hat{b}_{r\max 0})^2}{2} + \partial(b_{u\max} + b_{r\max}) \\ & +\frac{\bar{X}_1^2}{2\sigma_{yu}} + \frac{\bar{X}_2^2}{2\sigma_{yr}} + \frac{1}{2}\bar{\varepsilon}_u^2 + \frac{1}{2}\bar{\varepsilon}_r^2\end{aligned} \tag{47}$$

Set $\lambda_1 = k_{ue} - \frac{1}{2} > 0$, $\lambda_2 = k_{re} - \frac{1}{2} > 0$, $\lambda_3 = \frac{\sigma_u}{2}$, $\lambda_4 = \frac{\sigma_r}{2}$, $\lambda_5 = \frac{\sigma_{bu}}{2}$, $\lambda_6 = \frac{\sigma_{br}}{2}$, $\lambda_7 = A_u - \frac{\sigma_{yu}}{2} > 0$, $\lambda_8 = A_r - \frac{\sigma_{yr}}{2} > 0$ and

$$\begin{aligned}\Delta = & \sigma_u \frac{\left\|W_u - \hat{W}_u(0)\right\|^2}{2} + \sigma_r \frac{\left\|W_r - \hat{W}_r(0)\right\|^2}{2} \\ & +\sigma_{bu} \frac{(b_{u\max} - \hat{b}_{u\max 0})^2}{2} + \sigma_{br} \frac{(b_{r\max} - \hat{b}_{r\max 0})^2}{2} \\ & +\partial(b_{u\max} + b_{r\max}) + \frac{\bar{X}_1^2}{2\sigma_{yu}} + \frac{\bar{X}_2^2}{2\sigma_{yr}} + \frac{1}{2}\bar{\varepsilon}_u^2 + \frac{1}{2}\bar{\varepsilon}_r^2\end{aligned}$$

Then Eq. (47) becomes

$$\begin{aligned}\dot{V} \le & -k_{ze}z_e^2 - k_{\psi e}\psi_e^2 - \lambda_1 u_e^2 - \lambda_2 r_e^2 - \lambda_3 \left\|\tilde{W}_u\right\|^2 \\ & -\lambda_4 \left\|\tilde{W}_r\right\|^2 - \lambda_5 \tilde{b}_{u\max}^2 - \lambda_6 \tilde{b}_{r\max}^2 - \lambda_7 y_u^2 - \lambda_8 y_r^2 + \Delta\end{aligned} \tag{48}$$

Define

$\lambda := \min\{k_{ze}, k_{\psi e}, \lambda_1, \lambda_2, \lambda_3, \lambda_4, \lambda_5, \lambda_6, \lambda_7, \lambda_8\}$, then it follows form Eq. (48) that

$$\dot{V} \le -2\lambda V + \Delta \tag{49}$$

Solving inequality (49) gives

$$V \le (V(0) - \frac{\Delta}{2\lambda})e^{-2/t} + \frac{\Delta}{2\lambda} \le V(0)e^{-2/t} + \frac{\Delta}{2\lambda}, \forall t > 0.$$

The above inequality means that V is eventually bounded by $\frac{\Delta}{2\lambda}$. Thus all the error signals are uniformly ultimately bounded. In the case of appropriate parameters, the quantity $\frac{\Delta}{2\lambda}$ can be made arbitrarily small. Thus, the tracking errors may be made arbitrarily small.

In order to ensure the completeness of the proof of stability, the bounded dynamics of the sway velocity need to be analyzed. Construct the following Lyapunov function.

$$V_v = \frac{1}{2}m_{22}v^2 \tag{50}$$

According to Eq. (12), its time derivative is computed as

$$\begin{aligned}\dot{V}_v &= v(-m_{11}ur - d_{22}v + b_v) \\ &\le -d_{22}v^2 - m_{11}uvr + vb_v \\ &\le -d_{22}v^2 + \gamma_v v\end{aligned} \tag{51}$$

where $\gamma_v = \max[m_{11}|u||r| + |b_v|]$. Obviously, if $v > \gamma_v / d_{22}$ then $\dot{V}_v < 0$. Thus it can be concluded that the sway v is bounded.

6. Numerical Simulations

In this section, we will present three examples to illustrate the effectiveness and merits of the control scheme: Comparative examples with the result in Li et al. [25] and a classic PID controller [35]. For this purpose, the USV is selected as the Cybership 2, a 1:70 scale model of a supply vessel. For detail parameters, the readers can refer to [33-34]. The corresponding parameters we used are $m_{11} = 25.8$, $m_{22} = 33.8$, $m_{33} = 2.76$, $d_{11} = 0.72$, $d_{22} = 0.8896$, $d_{33} = 1.9$.

According to [11, 20], the external disturbances are considered as

$$\begin{cases} b_u = 0.5 + 0.1\sin(0.2t) + 0.3\cos(0.5t) \\ b_v = 0.5 + 0.2\sin(0.2t) + 0.1\cos(0.4t) \\ b_r = 0.5 + 0.1\sin(0.1t) + 0.1\cos(0.2t) \end{cases} \tag{52}$$

That is nonzero mean time-varying disturbance. In the simulation, the reference path is selected as

$$\begin{cases} x_d = 0.5t, y_d = 0, 0 \le t \le 100; \\ x_d = 50 + 0.5\cos(0.03(t-100)) \\ y_d = 0.5\sin(0.03(t-100)), t > 100. \end{cases} \tag{53}$$

Can be seen from the Eq. (53), the speed component along x-axis takes a constant value, and this situation is in line with the actual project.

The initial conditions of USV are

$$[x(0), y(0), \psi(0), u(0), v(0), r(0)]$$
$$= [-10m, -10m, 0rad, 0m/s, 0m/s, 0m/s]^{\cdot}$$

The control parameter is selected as $k_{ze} = 0.1$, $k_{\psi e} = 0.01$, $k_{ue} = 4$, $k_{re} = 40$, $\Gamma_u = 100$, $\sigma_u = 0.1$, $\Gamma_r = 100$, $\sigma_r = 0.1$, $\gamma_u = 1000$, $\sigma_{bu} = 0.01$, $\gamma_\tau = 1000$, $\sigma_{br} = 0.01$, $\partial = 0.1$ and the neural shunting model design parameters are taken as $A_1 = 5$, $B_1 = D_1 = A_u = 5 + f(\alpha_u) + g(\alpha_u)$, $A_2 = 5$, $B_2 = D_2 = A_r = 5 + f(\alpha_r) + g(\alpha_r)$.

Define $u_p = u_d - u$ and $r_p = r_d - r$.

The PID controller has the structure [35].

$$\tau_u = K_{Pu} u_p + \mathrm{K}_{Du} \dot{u}_p + \mathrm{K}_{Iu} \int_0^t u_p dt$$
$$\tau_r = K_{Pr} r_p + \mathrm{K}_{Dr} \dot{r}_p + \mathrm{K}_{Ir} \int_0^t r_p dt$$

Where τ_u and τ_r are the force and moment in the forward and steering directions, respectively. At the same time, the corresponding control parameters are selected as $K_{Pu} = 1100$, $K_{Du} = 90$, $K_{Iu} = 10$, $K_{Pr} = 80$, $K_{Dr} = 10$ and $K_{Ir} = 1$. The corresponding control laws of Li et al. [25] can refer to the original literature.

Remark 8. The expansion forms of $\dot{\alpha}_u$ and $\dot{\alpha}_r$ are shown in (40) and (44), respectively. If nothing is done, when designing the controller, $\dot{\alpha}_u$ and $\dot{\alpha}_r$ need to be fully deduced, and we can find that they are very complicated. For higher order systems, virtual control law needs to be repeated derivation. Such as [36], for a three order system, its virtual control law is derived two times, and its final control law is very complex. If neural shunting model is used, let α_u and α_r pass through (22) and (31), respectively. In the final control laws (26) and (35), β_u and β_r are needed without the need for $\dot{\alpha}_u$ and $\dot{\alpha}_r$. From this we can see that the problem of "explosion of complexity" is solved by introducing the neural shunting model. Besides, in essence, neural shunting model is a kind of filter. It can make the control signal flatten, which is beneficial to engineering application.

Remark 9. From the space point of view, neural shunting model can reduce the complexity of the control law. In the process of designing the controller, we can deeply appreciate the convenience of this simplification. Qualitative analysis from the point of view of time, a simple control law can save computation time (It is difficult to represent in simulation of this paper, and the neural shunting model will be used by the actual controller to quantify the time saved.). From the point of view of practical engineering, simple control algorithms mean that low configuration controllers can be selected, which can save costs.

Simulation results are plotted in Figs. 3-7. Fig. 3 shows the trajectory tracking in two-dimensional plane, where the reference path consists of straight line and a curve. It shows that in the presence of external disturbances and model uncertainty, the tracking results of the proposed strategy in this paper, the control strategy in Li et al. [25], and the PID control strategy. Meanwhile, the tracking performance of the proposed strategy and Li et al. [25] are better than PID. We can further see that the tracking effect of the proposed strategy is basically the same as that of Li et al. [25]. Fig. 4 demonstrates the position errors of three control strategies. We can find that the error convergence speed of the proposed strategy is obviously better than that of Li et al. [25]. Besides, the error of PID strategy is the worst, and the convergence is very slow. The reason is that the variables of the model are mutually coupled.

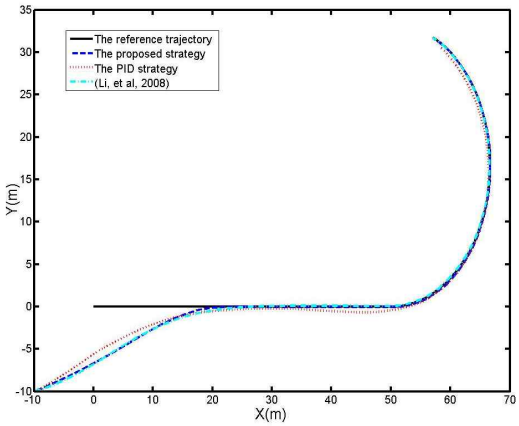

Fig. 3. Tracking trajectory

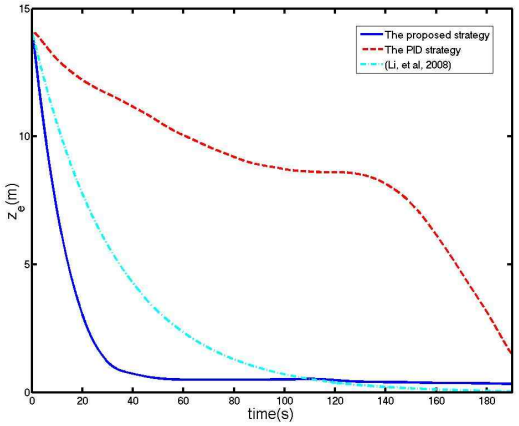

Fig. 4. Tracking errors

Figs. 5, 6 and 7 show the control forces and moments of each control strategy. Fig. 5 demonstrates the control inputs of the proposed control strategy. In the early stages, the maximum values of τ_u and τ_r are 300N and 1000N/m, respectively. They converge to a smaller value in a very short time, and compensate for the effects of external disturbances with smaller fluctuations. Fig. 6 demonstrates the control inputs of the control strategy in Li et al. [25]. In the early stages, its maximum values of τ_u and τ_r are obviously larger than the values of the proposed control strategy, and in the relatively stable phase, its control inputs also have larger chattering. The reason lies in that as noted previously, the essence of neural shunting model

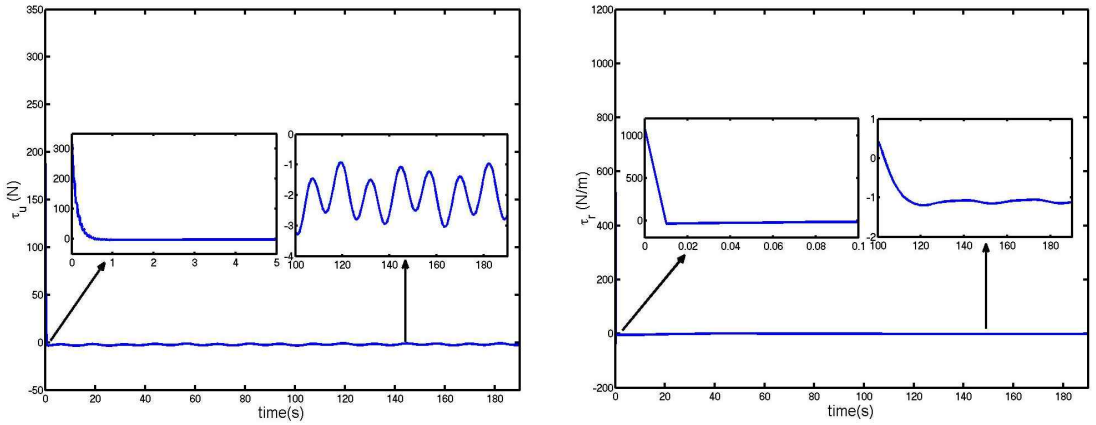

Fig. 5. Control inputs τ_u and τ_r (the proposed strategy)

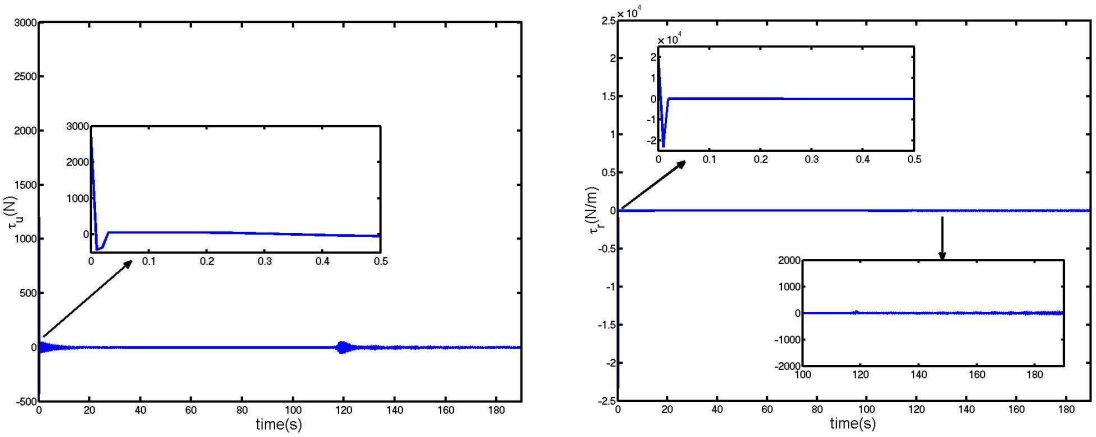

Fig. 6. Control inputs τ_u and τ_r (Li et al. [25])

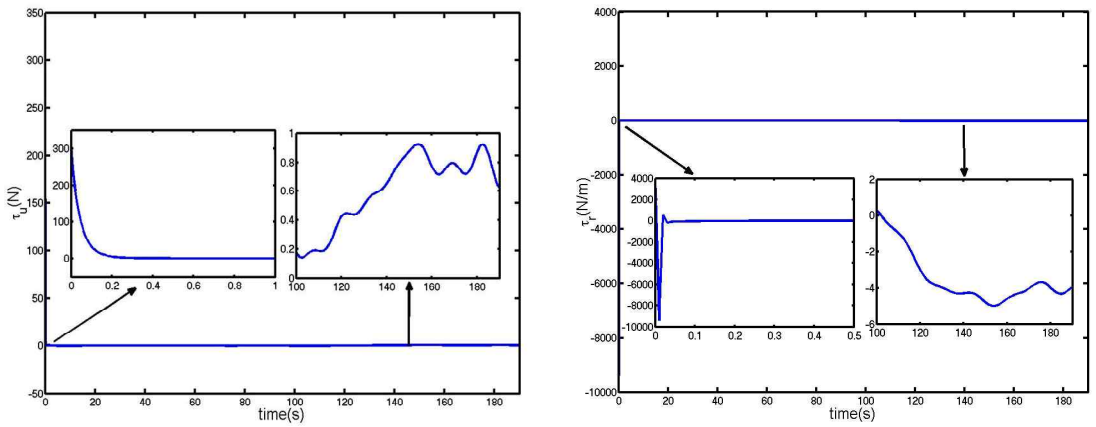

Fig. 7. Control inputs τ_u and τ_r (the PID strategy)

is a filtering, so it can make the system signal stationary. Neural shunting model is introduced into the design of trajectory tracking controller, so the control input of the proposed control strategy is more stable than that of Li et al. [25]. Fig. 7 shows the control inputs of the PID control strategy. The maximum values of its control inputs are larger than the proposed strategy. In other words, the control strategy proposed in this paper can save energy on the basis of ensuring the tracking effect.

7. Conclusion

In this paper, one focuses on tracking control for pod propulsion USV subject to unknown dynamics. On the basis of force analysis and assumption, the underactuated

characteristic of pod propulsion USV is proved by 3 DOFs MMG model. Then for the underactuated characteristic, in the case of unknown dynamics and external disturbance, the tracking control strategy is proposed. A novel neural shunting model is employed to solve the "explosion of complexity" problem of backstepping method. Furthermore, the universal approximation of neural network is used to solve the problem of model uncertainty and adaptive method is used to compensate for time-varying external disturbances. Finally, the UUB stability of all error signals has been proved using Lyapunov theory. Simulation results have been illustrated that the proposed algorithm can make the USV track the reference trajectory very well, which can also be used for the other practical underactuated system such as the nonholonomic robotics.

Even though, this work cannot attend to every detail of the control task, e.g., the algorithm may not account for the characteristic of propulsor. In other words, the final control laws are force and moment, not propulsion angle and propeller speed. Besides, from the point of view of quantitative analysis and practical engineering, how much computing time can save. The problems will be solved in the following works.

Acknowledgements

This work was supported by "the Nature Science Foundation of Liaoning Province of China" (grand number 2015020022), "the Nature Science Foundation of China" (grand number 51609033) and "the Fundamental Research Funds for the Central Universities" (grand numbers 3132014321, 3132016312 and 3132017133).

References

[1] Sinisterra A J, Dhanak M R and Ellenrieder K V, "Stereovision-based target tracking system for USV operations," *Ocean Engineering*, vol. 133, pp. 197-214, Feb. 2017.

[2] Song S H, Yoon Y H, Lee B K and Won C Y, "Autonomous Underwater Vehicles with Modeling and Analysis of 7-Phase BLDC Motor Drives," *Journal of Electrical Engineering & Technology*, vol. 9, no. 9, pp. 932-941, Sep. 2014.

[3] Mu D, Wang G, Fan Y and Zhao Y, "Modeling and Identification of Podded Propulsion Unmanned Surface Vehicle and Its Course Control Research," *Mathematical Problems in Engineering*, no. 4, pp. 1-13, Apr. 2017.

[4] Sonnenburg C R and Woolsey C A, "Modeling, Identification, and Control of an Unmanned Surface Vehicle," *Journal of Field Robotics*, vol. 30, no. 3, pp. 371-398, Mar. 2013.

[5] Jiang Z P, "Global tracking control of underactuated ships by Lyapunov's direct method," *Automatica*, vol. 38, no. 2, pp. 301-309, Feb. 2002.

[6] Do K D, Jiang Z P and Pan J, "Robust global stabilization of underactuated ships on a linear course: State and output feedback," *American Control Conference, 2002. Proceedings of the IEEE*, Anchorage, USA, Nov 2002.

[7] Do K D, Jiang Z P and Pan J, "Underactuated ship global tracking under relaxed conditions," *IEEE Transactions on Automatic Control*, vol. 47, no. 9. pp. 1529-1536, Sep. 2002.

[8] Ma B, "Global κ-exponential asymptotic stabilization of underactuated surface vessels," *Systems & Control Letters*, vol. 58, no. 3, pp. 194-201, Mar. 2009.

[9] Liao Y L, Wan L and Zhuang J Y, "Backstepping Dynamical Sliding Mode Control Method for the Path Following of the Underactuated Surface Vessel," *Procedia Engineering*, vol. 15, no. 7, pp. 256-263, Aug. 2011.

[10] Yang Y, Du J, Liu H, Guo C and Abraham A, "A Trajectory Tracking Robust Controller of Surface Vessels With Disturbance Uncertainties," *IEEE Transactions on Control Systems Technology*, vol. 22, no. 4, pp. 1511-1518, Jul. 2014.

[11] Zhang G, Zhang X and Zheng Y, "Adaptive neural path-following control for underactuated ships in fields of marine practice," *Ocean Engineering*, vol. 104, pp. 558-567, Jun. 2015.

[12] Liu L, Wang D and Peng Z, "Path following of marine surface vehicles with dynamical uncertainty and time-varying ocean disturbances," *Neurocomputing*, vol.173, pp.799-808, Aug. 2016.

[13] Peng Z, Wang D and Hu X, "Robust adaptive formation control of underactuated autonomous surface vehicles with uncertain dynamics," *Iet Control Theory & Applications*, vol. 5, no. 12, pp. 1378-1387, Aug. 2011.

[14] Tian Z, Li S, Wang Y and Wang X, "A Network Traffic Hybrid Prediction Model Optimized by Improved Harmony Search Algorithm," *Neural Network World*, vol.25, no.6, pp.669-685, Jun. 2015.

[15] Park B S, Kwon J W and Kim H, "Neural network-based output feedback control for reference tracking of underactuated surface vessels," *Automatica*, vol. 77, pp. 353-359, Jan. 2017.

[16] Chang W, Tong S and Li Y, "Adaptive fuzzy Backstepping output constraint control of flexible manipulator with actuator saturation," *Neural Computing & Applications*, pp.1-11, Jun. 2016.

[17] Tian Z, Li S and Wang Y, "TS fuzzy neural network predictive control for burning zone temperature in rotary kiln with improved hierarchical genetic algorithm," *International Journal of Modelling, Identification and Control*, vol. 25, no. 4, pp. 323-334, Jul. 2016.

[18] Tian Z, Gao X and Wang D, "The Application

Research of Fuzzy Control with Self-tuning of Scaling Factor in the Energy Saving Control System of Pumping Unit," *Engineering Letters*, vol. 24. no. 2, pp. 187-194, Feb. 2016.
[19] Tian Z, Li S, Wang Y and Zhang Q, "Multi Permanent Magnet Synchronous Motor Synchronization Control based on Variable Universe Fuzzy PI Method," *Engineering Letters*, vol. 23, no. 3. pp. 180-188, Mar. 2015.
[20] Pan C Z, Lai X Z, Yang S X and Wu M, "An efficient neural network approach to tracking control of an autonomous surface vehicle with unknown dynamics," *Expert Systems with Applications*, vol. 40, no. 5, pp. 1629-1635, Apr. 2013.
[21] Abbas H A, Belkheiri M and Zegnini B, "Feedback Linearization Control for Highly Uncertain Nonlinear Systems Augmented by Single-Hidden-Layer Neural Networks," *Journal of Engineering Science & Technology Review*, vol.8, no.2, pp.215-224, Feb. 2015.
[22] Do K D, "Practical control of underactuated ships," *Ocean Engineering*, vol. 37, no. 13, pp. 1111-1119, Sep. 2010.
[23] Krstic M, Kokotovic P V and Kanellakopoulos I, *Nonlinear and Adaptive Control Design:* John Wiley & Sons, Inc. 1995.
[24] Yang Y S and Wang X F, "Adaptive H∞ tracking control for a class of uncertain nonlinear systems using radial-basis-function neural networks," *Neurocomputing*, vol. 70, no. 4, pp. 932-941, Jan. 2007.
[25] Li J H, Lee P M, Jun B H and Lim Y K, "Point-to-point navigation of underactuated ships," *Automatica*, vol. 44, no. 12, pp. 3201-3205, Nov. 2008.
[26] Yang S X and Meng M, "An efficient neural network approach to dynamic robot motion planning," *Neural Networks*, vol. 13, no. 2, pp. 143-148, Mar. 2000.
[27] Du J, Hu X, Krstić M and Sun Y, "Robust dynamic positioning of ships with disturbances under input saturation," *Automatica*, vol. 73, pp. 207-214, Nov. 2016.
[28] Zeng B, "Research on Nonlinear Control of Waterjet Propulsion Surface Unmanned Naval vessel," *Harbin Engineering University*, 2012.
[29] Do K D and Pan J, "Robust adaptive path following of underactuated ships," *Automatica*, vol. 40, no. 6, pp. 929-944, Jun, 2004.
[30] Li T S, Wang D, Feng G and Tong S C, "A DSC Approach to Robust Adaptive NN Tracking Control for Strict-Feedback Nonlinear Systems," *IEEE Transactions on Systems Man & Cybernetics Part B*, vol. 40, no. 3, pp. 915-927, Jun. 2010.
[31] Chwa D, "Global Tracking Control of Underactuated Ships With Input and Velocity Constraints Using Dynamic Surface Control Method," *IEEE Transactions on Control Systems Technology*, vol. 19, no. 6, pp. 1357-1370, Nov. 2011.
[32] Do K D and Pan J, *Control of ships and underwater vehicles: design for underactuated and nonlinear marine systems:* Springer, 2009.
[33] Tee K P and Ge S S, "Control of fully actuated ocean surface vessels using a class of feed-forward approximators," *IEEE Transactions on Control Systems Technology*, vol. 14, no. 4, pp. 750-756, Jul. 2006.
[34] Dai S L, Wang C and Luo F, "Identification and learning control of ocean surface ship using neural networks," *IEEE Transactions on Industrial Informatics*, vol. 8, no. 4, pp. 801-810, Nov. 2012.
[35] Fossen T I, *Marine Control Systems: Guidance, Navigation, and Control of Ships rigs and underwater vehicles*: Marine Cybernetics, 2002.
[36] Du J L, Guo C and Yang C E, "Adaptive Nonlinear Design of autopilot for Ship Course Tracking," *Journal of Applied Science*, vol.24, no.1, pp.83-88, Jan. 2006.

Dong-Dong Mu He received the M.S. degree in Control theory and Engineering from Dalian Maritime University in 2015, and he is now pursuing his Ph.D. degree in control theory and control engineering at Dalian Maritime University. His research interests include modeling and intelligent control of unmanned surface vehicle.

Guo-Feng Wang He received the Ph.D. degree from Dalian Maritime University in 1996. He is currently a Professor in Dalian Maritime University, and his research interests include ship automation, advanced ship borne detection device and advanced power transmission.

Yun-Sheng Fan He received the Ph.D. degree from Dalian Maritime University in 2012. He is currently a Lecturer in Dalian Maritime University, and his research interests are ship intelligent control and its application.